

## Semiconductor electrodes. 26. Spectral sensitization of semiconductors with phthalocyanine

Calvin D. Jaeger, Fu-Ren F. Fan, and Allen J. Bard

*J. Am. Chem. Soc.*, **1980**, 102 (8), 2592-2598 • DOI: 10.1021/ja00528a012 • Publication Date (Web): 01 May 2002

Downloaded from <http://pubs.acs.org> on February 13, 2009

### More About This Article

---

The permalink <http://dx.doi.org/10.1021/ja00528a012> provides access to:

- Links to articles and content related to this article
- Copyright permission to reproduce figures and/or text from this article

- (21) M. H. Abraham and D. J. McLennan, *J. Chem. Soc., Perkin Trans. 2*, 873 (1977).  
 (22) Previously<sup>12</sup> we used the term "spurious" to describe this component of  $\Delta C_p^\ddagger$  derived strictly from kinetic complexity in contrast to those thermodynamic processes leading to maxima in  $\Delta C_p^\ddagger$  (e.g., see S. Leung and

E. Grunwald, *J. Phys. Chem.*, **74**, 687 (1970)). In this paper we substitute the term "abnormal  $\Delta C_p^\ddagger$ " to cover the combination of contributions from thermodynamic and kinetic complexity. We trust that this change will avoid the suggestion that the deviations in  $\Delta C_p^\ddagger$  with temperature are merely the consequences of experimental error.

## Semiconductor Electrodes. 26. Spectral Sensitization of Semiconductors with Phthalocyanine

Calvin D. Jaeger, Fu-Ren F. Fan, and Allen J. Bard\*

Contribution from the Department of Chemistry, The University of Texas at Austin, Austin, Texas 78712. Received August 16, 1979

**Abstract:** Spectral sensitization by metal-free phthalocyanine (H<sub>2</sub>Pc) films was observed on various semiconductor electrodes (single-crystal n-TiO<sub>2</sub>, n-SrTiO<sub>3</sub>, n-WO<sub>3</sub>, n-ZnO, n-CdS, n-CdSe, n-Si, and n-GaP; SnO<sub>2</sub> conducting glass). The spectral response of the sensitized photocurrent was generally the same as the absorption spectrum of the phthalocyanine. The rather thick (400 Å to 1 μm) H<sub>2</sub>Pc films showed both anodic and cathodic photocurrents depending upon the applied potential. The anodic photocurrents represented the usual sensitization of the n-type semiconductor, while the cathodic photocurrents were attributed to p-type behavior of the phthalocyanine itself. The current-potential curves of the semiconductor electrodes depended on the nature of the H<sub>2</sub>Pc film, the presence of a redox couple (i.e., *p*-hydroquinone/*p*-benzoquinone) in solution, and the wavelength of the irradiating light. The magnitude of the steady state sensitized photocurrent was linear with light intensity and was strongly affected by the addition of a supersensitizer.

### Introduction

Many studies have been conducted utilizing dyes to sensitize reactions at semiconductor and metal electrodes.<sup>1-5</sup> Such sensitization is of interest, because it provides information about the nature of charge transfer between excited states and electrodes and, from a more practical standpoint, because it allows the utilization of longer wavelength light to promote photoprocesses at semiconductors. The problem with utilizing dye sensitization to increase the efficiency of semiconductor processes arises primarily from the relatively low absorbance of the monolayer films of dyes adsorbed on the surface. This results in a very low overall quantum efficiency in terms of incident (rather than absorbed) light. The use of concentrated solutions of dyes (>10<sup>-4</sup> M) to maintain adsorbed monolayers can reduce the sensitized photocurrents, because the dye solution itself acts as a filter and thereby decreases the light intensity at the electrode surface. The use of thick, insoluble dye films<sup>6</sup> has generally not proven successful because of the high ohmic resistance of these films. Gerischer has, in fact, suggested that not much can be gained by using dye multilayers because of the ohmic resistance to electron transfer and an increased quenching probability.<sup>1</sup> With the exception of sensitization by adsorbed dyes on sintered zinc oxide electrodes,<sup>7</sup> the overall quantum efficiency for these processes is usually quite small. We report here spectral sensitization on semiconductor electrodes by thicker metal-free phthalocyanine (H<sub>2</sub>Pc) films (400 Å to 1 μm thick).

Sensitization by phthalocyanines is of interest for a number of reasons. Research on these materials has been very active recently,<sup>8</sup> and much is known about the redox behavior of these species in solution,<sup>9,10</sup> the catalytic activity of phthalocyanine electrodes (e.g., in fuel cells),<sup>11-13</sup> and their photoproperties.<sup>14-17</sup> These compounds have many characteristics which suggest that they might be useful sensitizers for semiconductor electrodes: (1) they absorb light strongly in the visible region of the solar spectrum; (2) a wide variety of small phthalocyanines have been prepared which allow a range of different compounds with different energy levels (i.e., redox potentials);

(3) many phthalocyanines are readily available, very stable, and insoluble in water; (4) the redox behavior of these compounds has been studied extensively; (5) the phthalocyanines often exhibit semiconducting behavior.

The initial studies reported in this paper concern the utilization of films of H<sub>2</sub>Pc primarily on single-crystal n-type semiconductors. The results are discussed according to a proposed mechanism of reactions of excited dye molecules on semiconductors<sup>1</sup> and the relative positions of the energy levels of the semiconductors, H<sub>2</sub>Pc and the redox couples in solution. The action spectra of the sensitized photocurrent and the current-potential (*i*-*V*) behavior are presented. The dependence of the sensitized photocurrent on light intensity and the concentration of a supersensitizer in solution is discussed. The stability of these systems both in the dark and under illumination and the p-type semiconductor properties of the H<sub>2</sub>Pc films are also described.

### Experimental Section

**Materials.** The metal-free phthalocyanine was purchased from Eastman (Rochester, N.Y.) and purified by repeated sublimation. The single-crystal semiconductors were obtained from several sources (CdSe and CdS, Cleveland Crystals; GaAs, GaP, and Si, Monsanto; ZnO and SrTiO<sub>3</sub>, Atomergic; TiO<sub>2</sub>, Fuji Titanium; WO<sub>3</sub>, Sandia). All of the semiconductors were n-type. Unless stated otherwise all other chemicals were reagent grade and the water had been triply distilled from an alkaline potassium permanganate solution. Ohmic contacts were made to the back of the semiconductors. An electrical contact was made to this ohmic contact using silver conducting paint (Acme Chemicals, New Haven, Conn.). On the back and sides, 5-min epoxy cement (Devcon Corp., Danvers, Mass.) was used to cover the electrode and mount the crystal to a glass tube.

The films were prepared by sublimation in a vacuum deposition apparatus (Vacuum Engineering Co., North Billerica, Mass.). The H<sub>2</sub>Pc was placed in a porcelain crucible. The H<sub>2</sub>Pc was heated under vacuum (10<sup>-5</sup>-10<sup>-6</sup> Torr) by means of a tungsten wire (0.060 in. in diameter). A current of 20 A, which corresponds to a crucible temperature of 400-450 °C, was passed through the wire. The electrode substrate was about 25 cm above the crucible. The film thicknesses of the sublimed H<sub>2</sub>Pc were determined by spectrophotometric

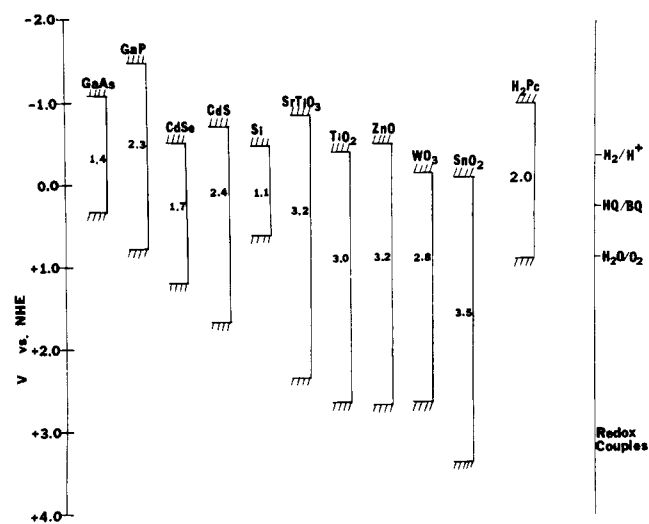


Figure 1. Relative energy levels of semiconductors,<sup>18</sup> H<sub>2</sub>Pc and redox couples; at pH 7, vs. NHE.

methods, while those of thick films (>5000 Å) were based upon the weight and density of H<sub>2</sub>Pc (1.5 g cm<sup>-3</sup>).<sup>8b</sup> The absorbance at 5750 Å was measured for a 5000-Å film and from the known thicknesses an absorption coefficient of  $4 \times 10^4$  cm<sup>-1</sup> was found. Other film thicknesses were estimated by comparing their absorbances with that of the 5000-Å film. From the absorption spectrum the deposited H<sub>2</sub>Pc is mainly in the  $\alpha$  form.

**Apparatus.** The electrochemical cell utilized a three-electrode system with a saturated calomel electrode (SCE) reference and a platinum wire separated by a glass frit as the counterelectrode. The cell had an optically flat Pyrex window on the side. Before all experiments the solutions were deaerated with prepurified nitrogen.

A PAR Model 173 potentiostat and PAR Model 175 universal programmer (Princeton Applied Research Corp., Princeton, N.J.) were used for the electrochemical experiments. The dc  $i$ - $V$  curves were recorded directly from the output of the potentiostat on to a Houston Instruments (Austin, Texas) Model 2000 X-Y recorder. The action spectra and the sensitized  $i$ - $V$  behavior were recorded using chopped light and a lock-in amplifier. Two different systems were used in these experiments. One system utilized a 2500-W xenon lamp and power supply (Schoffel Instrument Co., Westwood, N.J.), a monochromator (Jarrell-Ash, Waltham, Mass.), a PAR Model 192 variable frequency chopper, a PAR Model 5204 lock-in amplifier, and a Bascom-Turner 8110 recorder (Newton, Mass.). The other system used a 450-W xenon lamp and power supply (Oriol Corp., Stamford, Conn.), an Oriol monochromator, and a PAR HR8 lock-in amplifier. The light source used in the intensity and concentration studies was a Spectra Physics Model 132 He-Ne laser. All photocurrent-action spectra have been normalized against the power output of the lamp-monochromator.

## Results and Discussion

### Energy Levels and Mechanism for Photosensitized Currents.

The relative energy levels for the n-type semiconductors studied along with H<sub>2</sub>Pc and several redox couples are given in Figure 1. The Fermi level at the flat-band potential ( $V_{fb}$ ) for the semiconductors lies just below their respective conduction band (CB) edges. For bulk H<sub>2</sub>Pc the Fermi level is found slightly closer to the valence band (VB) ( $V_F = 0.5 \pm 0.1$ ,  $V_{CB} = -1.1 \pm 0.1$ , and  $V_{VB} = +0.8 \pm 0.1$  V vs. NHE).<sup>17</sup> The location of the energy levels of the H<sub>2</sub>Pc is relatively insensitive to pH<sup>19</sup> while those for most of the semiconductors shift with pH.<sup>18,20</sup> If not mentioned otherwise, all solutions were buffered at pH 7 (0.25 M phosphate buffer).

Both anodic and cathodic photocurrents attributable to light absorption by the H<sub>2</sub>Pc were observed with a given semiconductor, depending upon the applied potential. The observed anodic sensitized current depended upon the relative position of the energy levels of the semiconductor and H<sub>2</sub>Pc. For example, no anodic sensitization was observed for the n-GaP-

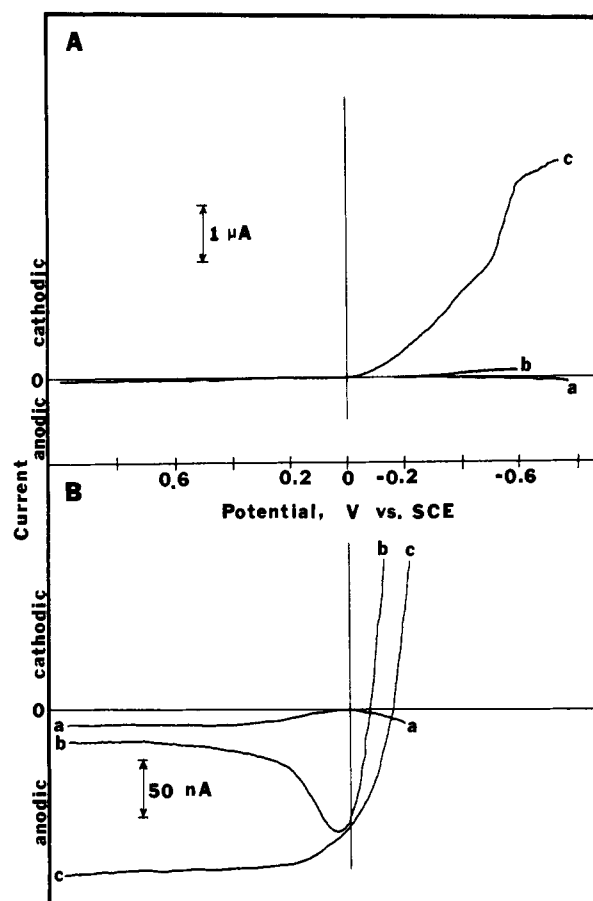
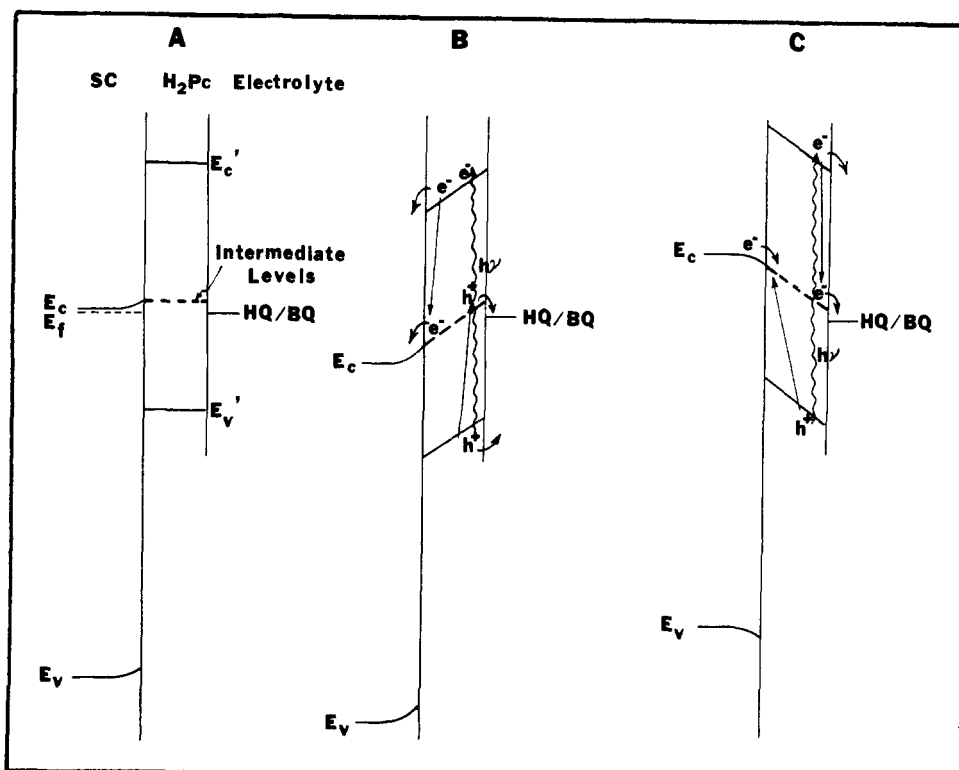


Figure 2. (A) Current-potential curves with a 0.5 M Na<sub>2</sub>SO<sub>4</sub>, 0.25 M phosphate buffer, illuminated with light ( $\lambda > 590$  nm): (a) WO<sub>3</sub> electrode without BQ; (b) WO<sub>3</sub>-H<sub>2</sub>Pc electrode without BQ; (c) WO<sub>3</sub>-H<sub>2</sub>Pc electrode with 8 mM BQ. Initial potential at zero-photocurrent potential. (B) Current-potential behavior in a 0.5 M Na<sub>2</sub>SO<sub>4</sub>, 0.25 M phosphate buffer, illuminated with light ( $\lambda > 590$  nm): (a) WO<sub>3</sub> electrode without HQ; (b) WO<sub>3</sub>-H<sub>2</sub>Pc electrode without HQ; (c) WO<sub>3</sub>-H<sub>2</sub>Pc electrode with 10 mM HQ. Initial potential at zero-photocurrent potential.

H<sub>2</sub>Pc electrode, because, as shown in Figure 1, the conduction band of GaP (at pH 7) lies above that of H<sub>2</sub>Pc. On the other hand, for the WO<sub>3</sub>-H<sub>2</sub>Pc electrode, an anodic sensitized current was observed in the presence of hydroquinone (HQ) beginning at a potential of  $\sim -0.1$  V vs. SCE and reaching a limiting value at more positive potentials. A cathodic photocurrent was found at more negative potentials with benzoquinone (BQ) (Figure 2). In this case, the respective Fermi levels of n-WO<sub>3</sub> and H<sub>2</sub>Pc are quite close with the conduction band edge of H<sub>2</sub>Pc lying above that of the WO<sub>3</sub>.

To help explain the experimental results, we first describe the proposed model for these photosensitized processes, as shown schematically in Figure 3. Because, for most of the cases discussed here, the H<sub>2</sub>Pc films were thin ( $\leq 400$  Å) and the carrier levels within these films were probably rather low, the space charge region at the H<sub>2</sub>Pc/semiconductor interface extends to the H<sub>2</sub>Pc/solution interface.<sup>21</sup> Thus a simplified parallelogram-shaped energy-level diagram (rather than a single Schottky barrier at the H<sub>2</sub>Pc/semiconductor interface) was assumed for the H<sub>2</sub>Pc phase. Such a constant field approximation has been used for even thicker films in solid-state photovoltaic cells with H<sub>2</sub>Pc.<sup>16</sup> When a sufficient positive potential is applied and the electrode is illuminated (with light of energy greater than the band gap energy ( $E_g$ ) of the H<sub>2</sub>Pc but lower than the  $E_g$  for the semiconductor), an anodic current is observed (Figure 3B). The electron-hole pair formed in the H<sub>2</sub>Pc film separates under the applied electric field and the electron migrates to the semiconductor/H<sub>2</sub>Pc interface



**Figure 3.** Representation of photosensitized electron transfer: (A) zero bias; (B) at positive applied potentials; (C) at negative applied potentials.  $E_c$ ,  $E_f$ , and  $E_v$  are the conduction band edge, the Fermi energy, and the valence band edge of semiconductors;  $E_c'$  and  $E_v'$  are the corresponding energies for  $H_2Pc$ .

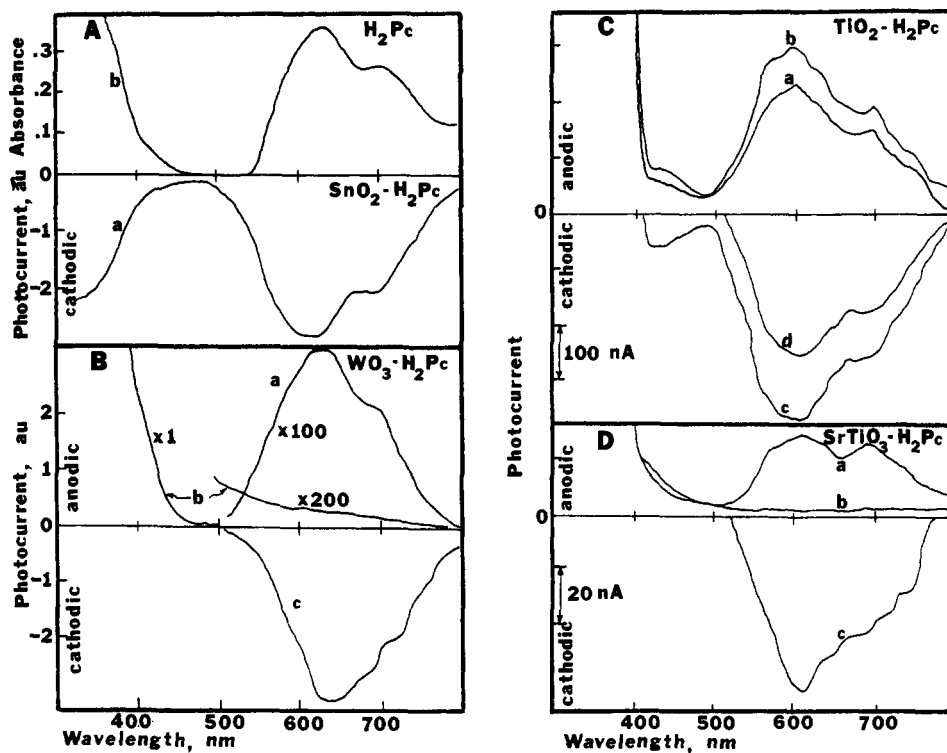


**Figure 4.** (A) (a) Photocurrent action spectrum for a  $SnO_2-H_2Pc$  electrode in 1 M KCl, 10 mM HQ,  $V = -0.6$  V vs. SCE; (b) absorption spectrum of  $H_2Pc$  on glass. (B) Photocurrent action spectrum for a  $WO_3-H_2Pc$  electrode in 0.5 M  $Na_2SO_4$  and 0.25 M phosphate buffer (pH 6.9): (a) anodic sensitization,  $V = +0.8$  V vs. SCE, with 50 mM HQ; (b) background photocurrent of a  $WO_3$  electrode; (c) cathodic sensitization,  $V = -0.7$  V vs. SCE, with 8 mM BQ. (C) Photocurrent action spectrum for a  $TiO_2-H_2Pc$  electrode in 1 M KCl: (a) anodic sensitization,  $V = +0.4$  V vs. SCE, with 10 mM HQ; (b) anodic sensitization,  $V = +0.2$  V vs. SCE, with 10 mM HQ; (c) cathodic sensitization,  $V = -1.0$  V vs. SCE; (d) cathodic sensitization,  $V = -0.4$  V vs. SCE. (D) Photocurrent action spectrum for a  $SrTiO_3-H_2Pc$  electrode in 1 M KCl: (a) anodic sensitization,  $V = -0.4$  V vs. SCE, with 10 mM HQ; (b) background photocurrent of a  $SrTiO_3$  electrode,  $V = -0.4$  V vs. SCE; (c) cathodic sensitization,  $V = -0.6$  V vs. SCE.

while the hole moves to the  $H_2Pc$  solution interface. An intermediate level has been proposed for phthalocyanine<sup>22</sup> and such a level may be involved both in mediating electron transfer

to the conduction band of the semiconductor and hole transfer to a redox couple in solution, as shown in Figure 3B. When a negative potential is applied under illumination, causing band

structure shown in Figure 3C to exist, a cathodic photosensitized current is observed. In this case, holes created within the  $H_2Pc$  migrate toward the substrate semiconductor while the electrons move to the solution interface. With a negative bias the applied potential causes the bands in the semiconductor to bend downward, producing degeneracy at the surface of the n-type semiconductor. Its behavior approaches that of a metal and the observed photoeffects are due solely to the  $H_2Pc$ . The photogenerated holes in the  $H_2Pc$  can recombine with the electrons from the semiconductor either through the intermediate level or via the valence band of  $H_2Pc$ . Cathodic photocurrents on phthalocyanine-metal electrodes have been reported previously.<sup>15</sup> The redox couple (HQ/BQ) acts as a supersensitizer.<sup>1</sup>

#### Photocurrent-Wavelength Response. Oxide Semiconductors.

The anodic and cathodic photocurrent action spectra for the oxide semiconductor- $H_2Pc$  electrodes are shown in Figure 4. All curves represent irradiation with modulated light (100 Hz) and phase-sensitive detection. In general, at applied potentials positive of the  $V_{fb}$  of the semiconductor the photosensitized currents were anodic, while at potentials negative of  $V_{fb}$  the photosensitized currents were cathodic. For example, for  $H_2Pc$  on  $SnO_2$  conducting glass (Figure 4A), the  $SnO_2$  glass acts only as a contact and the cathodic photoeffect is due solely to the  $H_2Pc$ . The photocurrent action spectrum (a) is very similar to the absorption spectrum of  $H_2Pc$  on glass (b). For the  $SnO_2$ - $H_2Pc$  electrodes, as the applied potential was made more positive, the intensity of the cathodic photocurrent decreased. As shown in Figure 3, at more positive potentials a larger barrier for electron transfer from the  $SnO_2$  to the  $H_2Pc$  would be present. Generally, as shown in Figure 4, both the anodic and cathodic photosensitized currents with the other wide band gap oxide semiconductor- $H_2Pc$  electrodes were all close to the absorption spectrum of  $H_2Pc$ . For the  $TiO_2$  and  $SrTiO_3$ - $H_2Pc$  electrodes, the magnitude of the photosensitized current was potential dependent. The cathodic photocurrent decreased as the applied potential was made more positive. Moreover, at a given potential just positive of the  $V_{fb}$  of  $TiO_2$  (or  $SrTiO_3$ ), a cathodic photosensitized current was observed at longer wavelengths ( $\lambda > 500$  nm) and an anodic photocurrent due to the band gap excitation of the  $TiO_2$  (or  $SrTiO_3$ ) was found at shorter wavelengths ( $\lambda < 450$  nm). Thus with the  $TiO_2$  and  $SrTiO_3$ - $H_2Pc$  electrodes there is a small potential region near  $V_{fb}$  where the energetics are favorable for electron transfers either to or from the  $H_2Pc$ .

**Current-Potential Behavior. Oxide Semiconductors.** Generally, all of the oxide semiconductor- $H_2Pc$  electrodes showed similar  $i-V$  behavior (see Figures 2 and 5). For example, in Figure 5  $i-V$  curves for  $TiO_2$  and  $TiO_2$ - $H_2Pc$  electrodes for a 10 mM HQ solution under illumination with chopped light are compared. The light was chopped to show the difference between the dark and the photocurrent. The photoresponse of the  $TiO_2$ - $H_2Pc$  electrode under irradiation with light of energy less than the  $E_g$  for  $TiO_2$  (i.e., with a yellow filter, Oriol G 772-4750, 50% transmittance,  $T$ , at 500 nm and  $< 1\%$   $T$  at 465 nm) is shown in Figure 5d. At negative potentials a cathodic photocurrent is observed due to the  $H_2Pc$ . At positive potentials, only a small photoanodic current attributable to  $H_2Pc$  sensitization is found. Moreover, there is a potential region of about 0.2 V ( $-0.225$  to  $-0.425$  V vs. SCE) where anodic and cathodic photocurrents under white-light illumination are possible (depending on whether HQ or BQ is present in the solution), an anodic photocurrent due to the  $TiO_2$  absorption and a cathodic photocurrent from the  $H_2Pc$ . As shown in Figure 5c, for the  $TiO_2$ - $H_2Pc$  electrode in the presence of HQ an anodic spike is observed at potentials positive of  $V_{fb}$  when the electrode is illuminated; such a spike is not found on an uncoated  $TiO_2$  electrode in the presence of HQ (Figure 5b). This anodic spike can be attributed to photooxidation of  $H_2Pc$

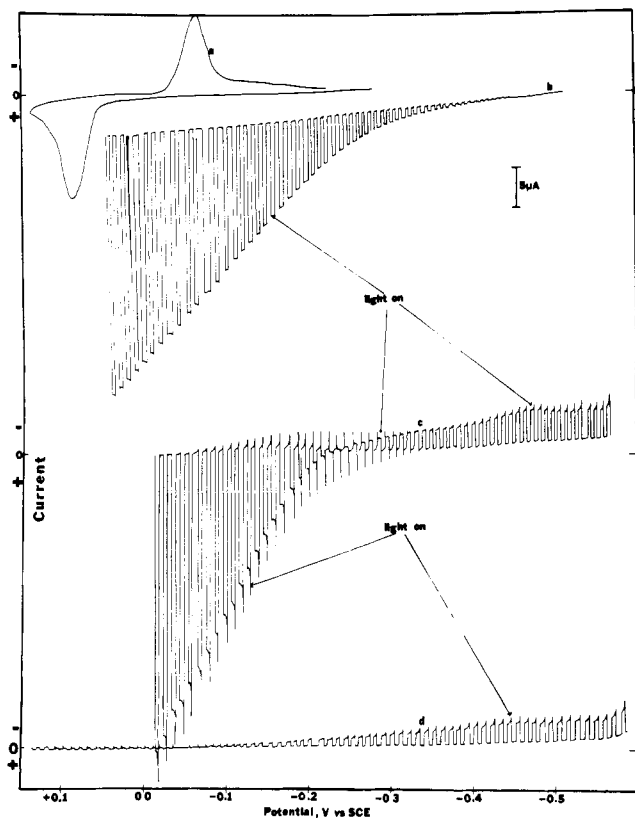


**Figure 5.** Current-potential curves with a HCl, NaCl, 10 mM HQ (pH 3.7) solution: (a) cyclic voltammogram of HQ/BQ on a Pt disk electrode; (b)  $TiO_2$  electrode illuminated with chopped white light; (c)  $TiO_2$ - $H_2Pc$  electrode illuminated with chopped white light; (d)  $TiO_2$ - $H_2Pc$  electrode illuminated with chopped light ( $\lambda > 465$  nm).

at the  $TiO_2$ - $H_2Pc$  interface by holes photogenerated in the  $TiO_2$ . This oxidized  $H_2Pc$  is reduced by the solution HQ, but this rate may be sluggish because of the poor mobility of the charge carriers in  $H_2Pc$ .<sup>24b</sup> When the light is turned off, a cathodic dark current spike is observed at potentials between about 0.0 and  $-0.325$  V vs. SCE. The dark cathodic current spike might involve the back electron transfer from  $TiO_2$  to the photooxidized  $H_2Pc$  and the reduction of BQ to HQ generated during the illumination period. Note that reduction of BQ to HQ is possible at potentials negative of 0 V vs. SCE, as shown by the  $i-V$  curve at Pt (Figure 5a). Such dark reduction processes do not occur at the uncoated  $TiO_2$  electrode following photooxidation (Figure 5b). This suggests that the  $H_2Pc$  on the electrode surface provides surface states or an intermediate level for this back electron transfer. Such behavior has been observed for other semiconductor electrodes.<sup>23</sup>

The  $i-V$  curves for the  $WO_3$ - $H_2Pc$  electrodes during illumination with light of less energy than  $E_g$  of  $WO_3$  (i.e.,  $\lambda > 590$  nm) at potentials negative of  $V_{fb}$  show that the cathodic photocurrent is strongly affected by the presence of benzoquinone (Figure 2A(c)). In the case of the anodic sensitized photocurrent (Figure 2B), the presence of hydroquinone (HQ) affects the photocurrent-potential behavior. Without HQ during a potential sweep, the anodic sensitized photocurrent reaches a maximum at about  $+0.05$  V vs. SCE and then decreases, probably because the  $H_2Pc$  itself is oxidized. In the presence of HQ the sensitized photocurrent reaches a limiting value which is related to the concentration of HQ and its diffusion to the electrode surface.

#### Dependence of Sensitized Photocurrent on Light Intensity.

The dependence of the sensitized photocurrent for the oxidation of HQ on light intensity for the  $TiO_2$ - $H_2Pc$  (a) and  $WO_3$ - $H_2Pc$  (b, c) electrodes is shown in Figure 6. In both cases

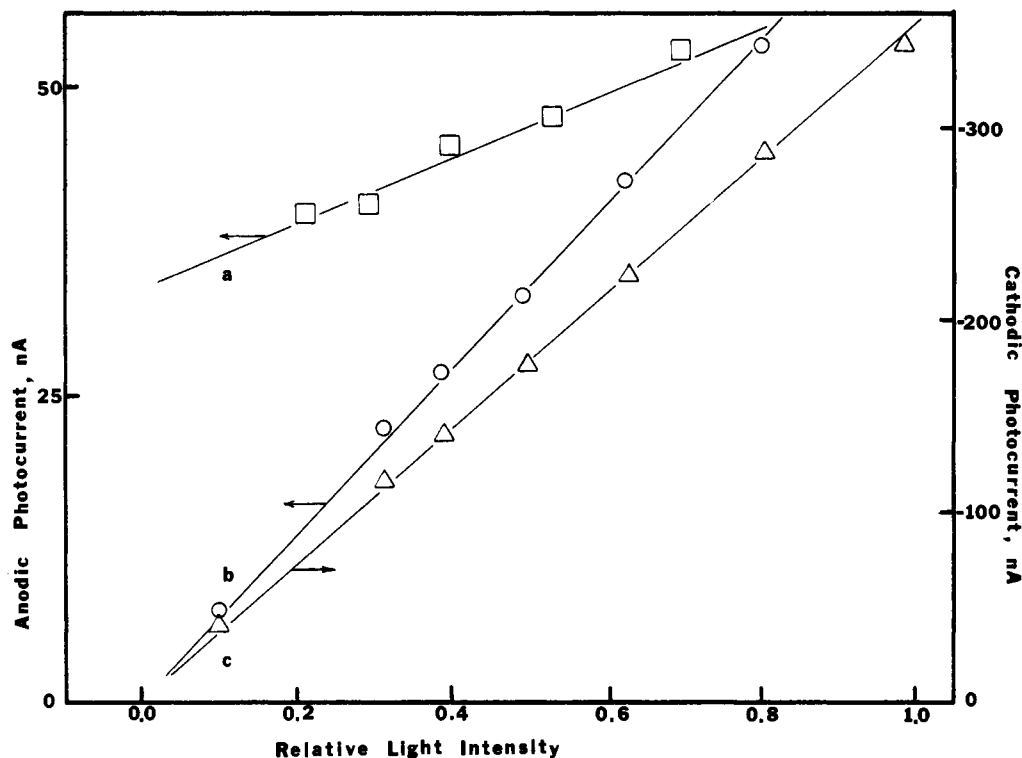


**Figure 6.** Dependence of sensitized photocurrent on light intensity, 1.7-mW He-Ne laser (632.8 nm): (a)  $\text{TiO}_2\text{-H}_2\text{Pc}$  electrode in 1 M KCl with 10 mM HQ,  $V = +0.4$  V vs. SCE; (b)  $\text{WO}_3\text{-H}_2\text{Pc}$  electrode in 0.5 M  $\text{Na}_2\text{SO}_4$ , 0.25 M phosphate buffer (pH 7), with 50 mM HQ,  $V = +0.8$  V vs. SCE; (c)  $\text{WO}_3\text{-H}_2\text{Pc}$  electrode in 0.5 M  $\text{Na}_2\text{SO}_4$ , 0.25 M phosphate buffer (pH 7), with 8 mM BQ,  $V = -0.7$  V vs. SCE.

the photocurrent depends linearly on light intensity.<sup>24a</sup> These experiments were conducted with a He-Ne laser (1.7 mW, 632.8 nm) and neutral density filters to vary the light intensity. Based upon the maximum photocurrent ( $i_p$ ) for a  $\text{WO}_3\text{-H}_2\text{Pc}$  (400 Å) electrode, the incident quantum efficiency,  $\phi$ , was calculated for both the anodic and cathodic sensitization, by dividing the current flow by the incident light flux. The monochromatic quantum efficiencies in terms of incident radiation were  $\phi_a = 7.61 \times 10^{-5}$  for the anodic photocurrent ( $i_p = 66$  nA) and  $\phi_c = 4.03 \times 10^{-4}$  for the cathodic photocurrent ( $i_p = 350$  nA). The efficiencies in terms of absorbed photons,  $\phi_a'$  and  $\phi_c'$ , are about  $1.6 \times 10^{-4}$  and  $8.48 \times 10^{-4}$ , respectively. The values for  $\phi_a'$  and  $\phi_c'$  are based upon an absorbance of  $7 \times 10^4 \text{ cm}^{-1}$  for the 400 Å thick  $\text{H}_2\text{Pc}$  film. These low efficiencies indicate that considerable recombination must be occurring.

**Dependence of Sensitized Photocurrent on Concentration of HQ/BQ.** The steady state  $\text{H}_2\text{Pc}$ -sensitized photocurrent depended upon the addition of a suitable supersensitizer (Figure 7). Thus, for  $\text{WO}_3$  at positive potentials, the addition of a small amount of HQ sharply increased the anodic photocurrent (curve a). A similar dependency was observed with  $\text{TiO}_2$  (curve c). After this sharp increase at low concentrations, the current tended to level off, suggesting that internal electron-hole pair recombination, rather than the oxidation of the  $\text{H}_2\text{O}$ , was governing the current. A similar effect was observed for the cathodic photosensitized current at  $\text{WO}_3$  (curve b). The sensitized photocurrents of the oxide semiconductors remained constant under extended irradiation. For example, the photocurrents at  $\text{WO}_3\text{-H}_2\text{Pc}$  remained constant for at least 3 h in the presence of HQ or BQ (Figure 8). Note that in this experiment the cathodic photocurrent was over 100 times larger than the anodic one. Similar stability was also found for  $\text{H}_2\text{Pc}$  films on  $\text{TiO}_2$  and  $\text{SnO}_2$ .

**$\text{H}_2\text{Pc}$  Films on Small Band-Gap Semiconductors.** The behavior of semiconductors with  $E_g$  values smaller than that of  $\text{H}_2\text{Pc}$  was also investigated. The primary motivation for these

studies was the possibility that films of  $\text{H}_2\text{Pc}$  might stabilize the semiconductors from anodic photodissolution; previous attempts at such stabilization of semiconductors with metal<sup>25,26</sup> or  $\text{TiO}_2$ <sup>27,28</sup> films have been reported. Photosensitized cathodic currents attributable to  $\text{H}_2\text{Pc}$  could be observed, e.g., with n-Si (Figure 9c); in this case the semiconductor again behaved as a contact to the  $\text{H}_2\text{Pc}$  film. The observed action spectra were somewhat broader than that predicted by the absorption spectrum of  $\text{H}_2\text{Pc}$ . For n-GaAs (Figure 9a) anodic photosensitization would not be expected, since it absorbs light of longer wavelength than  $\text{H}_2\text{Pc}$ . In this case the  $\text{H}_2\text{Pc}$  layer merely acted as a filter so that the observed anodic photoreponse was smaller with the  $\text{H}_2\text{Pc}$  film than in its absence.

We found no long-term stabilization of the semiconductors CdS, CdSe, and GaP from photocorrosion by coating with even rather thick (1–1.5  $\mu\text{m}$ )  $\text{H}_2\text{Pc}$  films under conditions where the bare electrodes corrode. The evidence for such instability of coated electrodes consisted of the decreased photocurrents under intense band gap illumination ( $>100 \text{ mW/cm}^2$ ) for extended periods (longer than 4 h) and the production of photocorrosion products on the electrode surface. We suggest, in line with previous studies involving coatings with  $\text{TiO}_2$ ,<sup>27,28</sup> that the films have small holes or cracks which eventually allow decomposition reactions of the substrate semiconductor. Additional evidence for incomplete coverage by the  $\text{H}_2\text{Pc}$  film is the observed shift in the potential for photosensitized anodic current onset with pH over a pH range of 1–9 ( $\sim 63 \pm 5 \text{ mV/pH unit}$ ) for  $\text{H}_2\text{Pc}$ -coated  $\text{WO}_3$ ,  $\text{SrTiO}_3$ , and  $\text{TiO}_2$  electrodes. Such a shift would appear unlikely for  $\text{H}_2\text{Pc}$  itself and signals some kind of involvement of the substrate material even for the photosensitized process.

## Conclusions

The photosensitization of semiconductor electrodes by metal-free phthalocyanine films has been clearly shown. The action spectrum of the sensitized photocurrent of semiconductor- $\text{H}_2\text{Pc}$  electrodes where both anodic and cathodic

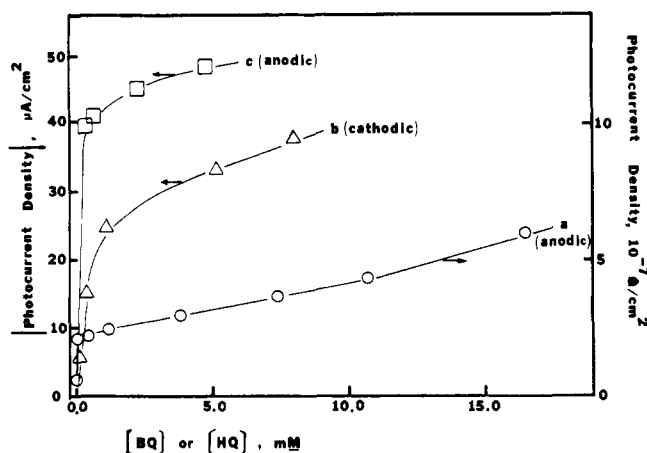


**Figure 7.** Dependence of sensitized photocurrent on concentration of HQ/BQ: (a)  $\text{WO}_3\text{-H}_2\text{Pc}$  electrode in 0.5 M  $\text{Na}_2\text{SO}_4$  and 0.25 M phosphate buffer (pH 7), with HQ,  $V = +0.8$  V vs. SCE; (b)  $\text{WO}_3\text{-H}_2\text{Pc}$  electrode in 0.5 M  $\text{Na}_2\text{SO}_4$  and 0.25 M phosphate buffer (pH 7), with BQ,  $V = -0.7$  V vs. SCE; (c)  $\text{TiO}_2\text{-H}_2\text{Pc}$  electrode in 1 M KCl with HQ,  $V = +0.4$  V vs. SCE.

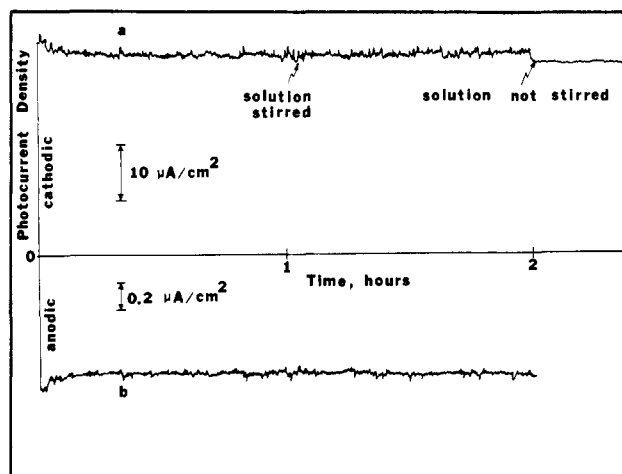


**Figure 8.** Stability of sensitized photocurrent in 0.5 M  $\text{Na}_2\text{SO}_4$ , 0.25 M phosphate buffer (pH 7), light ( $\lambda > 590$  nm),  $\text{WO}_3\text{-H}_2\text{Pc}$  electrode: (a) cathodic sensitized photocurrent, with 8 mM BQ,  $V = -0.7$  V vs. SCE; (b) anodic sensitized photocurrent, with 50 mM HQ,  $V = +0.8$  V vs. SCE.

photocurrents are observed generally compares well with the absorption spectrum of  $\text{H}_2\text{Pc}$ . The sign of the photocurrent depends upon the applied potential. At potentials very positive of  $V_{fb}$  the effect is anodic and at very negative potentials it is cathodic. This effect is similar to that found by Honda et al.<sup>15b</sup> for films of metal phthalocyanines on semiconductors. The  $i$ - $V$  curves show that the presence of the  $\text{H}_2\text{Pc}$ , and also of hydroquinone, markedly affects the behavior of an illuminated semiconductor electrode. The observation of dark cathodic peaks suggests the presence of some intermediate level within the band gap of the semiconductor- $\text{H}_2\text{Pc}$  electrode. Generally, the dependence of the sensitized photocurrent on light intensity and concentration of the supersensitizer follows the behavior previously shown for dye sensitization on semiconductor electrodes. Although the quantum efficiencies for the observed photosensitized processes were small and we were unsuccessful in stabilizing small band gap semiconductors with such films, for the reasons listed in the Introduction, phthalocyanines remain of interest for sensitizing semiconductor photoprocesses. Work is continuing in this laboratory utilizing metal phthalocyanines with other p- and n-type semiconductor electrodes.

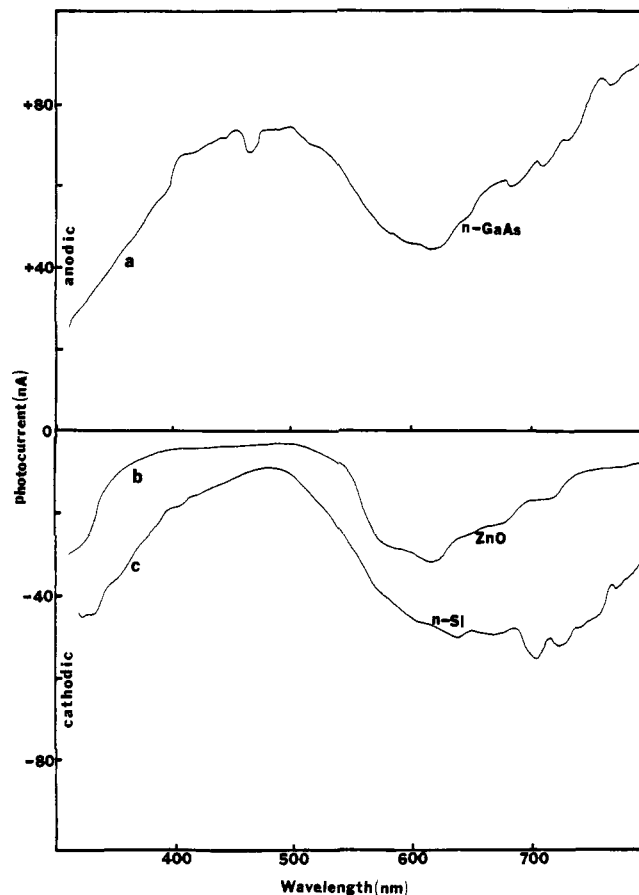


**Figure 9.** Action spectra for (a) anodic photocurrent at  $\text{n-GaAs-H}_2\text{Pc}$ , 1 M KCl, 10 mM HQ,  $V = -0.6$  V vs. SCE; (b) cathodic photocurrent at  $\text{n-ZnO-H}_2\text{Pc}$ , 1 M KCl, 10 mM BA,  $V = -1.0$  V vs. SCE; (c) as (b) for  $\text{n-Si-H}_2\text{Pc}$ ,  $V = -1.0$  V vs. SCE.

**Acknowledgment.** The support of this research, which is a joint project with Professor A. B. P. Lever of York University, by the Office of Naval Research is gratefully acknowledged.

## References and Notes

- (1) Gerischer, H.; Willig, F. *Top. Curr. Chem.* **1969**, *61*, 31, and references cited therein.
- (2) Spittler, M. T.; Calvin, M. *J. Chem. Phys.* **1977**, *66*, 4294.
- (3) Gerischer, H. *Photochem. Photobiol.* **1975**, *16*, 243, and references cited therein.
- (4) Memming, R. *Photochem. Photobiol.* **1975**, *16*, 325, and references cited therein.
- (5) Fujishima, A.; Iwase, I.; Honda, K. *J. Am. Chem. Soc.* **1976**, *98*, 1625, and references cited therein.
- (6) Tsubomura, H.; Matsumura, M.; Nomura, Y.; Amamiya, T. *Nature (London)* **1976**, *261*, 402.
- (7) Matsumura, M.; Nomura, Y.; Tsubomura, H. *Bull. Chem. Soc. Jpn.* **1977**, *50*, 2533.
- (8) (a) Tachikawa, H.; Faulkner, L. R. *J. Am. Chem. Soc.* **1978**, *100*, 4399. (b) Fan, F.-R.; Faulkner, L. R. *J. Chem. Phys.* **1978**, *69*, 3334, and references cited therein.
- (9) Clack, D. W.; Hush, N. S.; Woolsey, I. S. *Inorg. Chim. Acta* **1976**, *19*, 129.
- (10) Wolberg, A.; Manassen, J. *J. Am. Chem. Soc.* **1970**, *92*, 2982.
- (11) Appleby, A. J.; Savy, M. *Electrochim. Acta* **1976**, *21*, 9567.
- (12) Loutfy, R. O.; Sharp, J. H. *J. Appl. Electrochem.* **1977**, *7*, 315.
- (13) Sen, R. K.; Zagal, J.; Yeager, E. *Inorg. Chem.* **1977**, *16*, 3376.
- (14) Papovic, Z. D.; Sharp, J. H. *J. Chem. Phys.* **1977**, *66*, 5076.
- (15) (a) Meshitsuka, S.; Tamaru, K. *J. Chem. Soc., Faraday Trans. 1* **1977**, *73*, 236; **1977**, *73*, 760. (b) Minami, N.; Watanabe, T.; Fujishima, A.; Honda, K. *Ber. Bunsenges. Phys. Chem.* **1979**, *83*, 476.
- (16) Hall, K. J.; Bonham, J. S.; Lyons, L. E. *Aust. J. Chem.* **1978**, *31*, 1661.
- (17) Fan, F.-R.; Faulkner, L. R. *J. Am. Chem. Soc.* **1979**, *101*, 4779.
- (18) Nozick, A. J. *Annu. Rev. Phys. Chem.* **1978**, and references cited therein.
- (19) The onset potential of the photooxidation of hydroquinone on  $\text{H}_2\text{Pc}$ -coated platinum electrodes has been found to be pH independent in the pH range 2-9.5, at about 0.3 V vs. SCE.
- (20) Watanabe, T.; Fujishima, A.; Honda, K. *Chem. Lett.* **1974**, 897.
- (21) The width of the space charge layer of phthalocyanine thin films might be

- several hundred ångströms. See: ref 8b or Ghosh, A. K.; Morel, D. L.; Feng, T.; Shaw, R. F.; Rowe, C. A. *J. Appl. Phys.* **1974**, *45*, 230.
- (22) Fan, F.-R. F. Dissertation, University of Illinois, 1978.
- (23) Kohl, P. A. Ph.D. Dissertation, The University of Texas at Austin, 1978.
- (24) (a) Meier, H. "Organic Semiconductors"; Verlag Chemie: Weinheim/Bergstr., West Germany, 1974. (b) Gutman, F.; Lyons, L. E. "Organic

- Semiconductors"; Wiley: New York, 1967.
- (25) Nakato, Y.; Ohnishi, T.; Tsubomura, H. *Chem. Lett.* **1975**, 883.
- (26) Wilson, R. H.; Harris, L. A.; Gerstner, M. E. *J. Electrochem. Soc.* **1977**, *124*, 1233.
- (27) Kohl, P.; Frank, S. N.; Bard, A. J. *J. Electrochem. Soc.* **1977**, *124*, 225.
- (28) Tomkiewicz, M.; Woodall, J. *J. Electrochem. Soc.* **1977**, *124*, 1436.

## Charge-Transfer Absorptions of Cu(II)-Imidazole and Cu(II)-Imidazolate Chromophores

Timothy G. Fawcett, Ernest E. Bernarducci, Karsten Krogh-Jespersen,\* and Harvey J. Schugar\*

Contribution from the Department of Chemistry, Rutgers, The State University of New Jersey, New Brunswick, New Jersey 08903. Received August 20, 1979

**Abstract:** Electronic spectra over the 50 000–20 000-cm<sup>-1</sup> region are reported for well-characterized chromophores having Cu(II)-imidazole (ImH) and Cu(II)-imidazolate (Im<sup>-</sup>) units. For tetragonal Cu(II)-ImH chromophores, three ligand to metal charge-transfer (LMCT) absorptions originate from the  $\sigma$ -symmetry nitrogen donor lone pair and from two  $\pi$ -symmetry ring orbitals, one having primarily carbon character ( $\pi_1$ ) and the other having primarily nitrogen character ( $\pi_2$ ). These  $\sigma(\text{ImH}) \rightarrow \pi_2(\text{ImH})$ ,  $\pi_2(\text{ImH}) \rightarrow \pi_1(\text{ImH})$ , and  $\pi_1(\text{ImH}) \rightarrow \text{Cu(II)}$  LMCT absorptions occur at  $\sim 220$ ,  $\sim 260$ , and  $\sim 330$  nm, respectively. Ligand rotation causes the  $\pi$ -symmetry absorptions to be broadened for solutions containing geometrically unconstrained Cu(II)-ImH complexes. The  $\pi$ -symmetry absorptions generally are well-resolved spectral features of crystalline complexes, and may be split when the ImH groups have nonequivalent orientations. The  $\sigma(\text{ImH}) \rightarrow \text{Cu(II)}$  absorption at 220 nm is insensitive to ligand rotation about the Cu-N axis, and is well resolved from the ligand-localized absorption at  $\sim 205$  nm. The Cu(II)-Im<sup>-</sup> complexes exhibit an additional and characteristic broad absorption at  $\sim 375$  nm for which a tentative assignment has been suggested. Tetragonal type 2 and type 3 copper protein chromophores are expected to exhibit corresponding  $\pi(\text{ImH}) \rightarrow \text{Cu(II)}$  LMCT transitions in the near-UV region. Such absorptions are expected to be red shifted for the approximately tetrahedral type 1 copper chromophores. The reported spectra of the above types of proteins briefly are reconsidered from this point of view.

### Introduction

Imidazole groups have important ligand roles when copper is complexed by histidine-containing peptides. The structural features of such bonding have been well characterized by X-ray crystallographic studies of low molecular weight Cu(II) complexes<sup>1</sup> and of proteins such as plastocyanin,<sup>2</sup> azurin,<sup>3</sup> and superoxide dismutase.<sup>4</sup> Other evidence has been used to infer Cu(II)-imidazole interactions in stellacyanin,<sup>5</sup> serum albumin,<sup>6</sup> galactose oxidase,<sup>7</sup> cytochrome *c* oxidase,<sup>8</sup> ceruloplasmin,<sup>9</sup> hemocyanins,<sup>10</sup> and other proteins. Our interest in the electronic spectra of the Cu(II) proteins has led to the synthesis and/or characterization of model complexes which have served to elucidate features of Cu(II)-thioether,<sup>11</sup> Cu(II)-disulfide,<sup>12</sup> Cu(II)-mercaptide,<sup>13</sup> Cu(II)-deprotonated amide,<sup>14</sup> and Cu(II)-superoxide<sup>15</sup> bonding. We report here an extension of these studies to the ligand to metal charge-transfer (LMCT) absorptions of Cu(II)-imidazole (ImH) and Cu(II)-imidazolate (Im<sup>-</sup>) chromophores. Charge-transfer spectra of fully characterized low molecular weight Cu(II) complexes are presented and assigned. The presence of corresponding absorptions in the spectra of Cu(II) proteins is discussed briefly.

### Experimental Section

**Preparation of Complexes.** Imidazole (ImH) and L-histidine were obtained from the Aldrich Chemical Co. and Matheson Coleman and Bell, respectively. These ligands were purified by recrystallization (thrice) from water that was distilled and deionized. The water used for recrystallization and spectral studies must be scrupulously pure. Otherwise, the spectra of the free ligands and Zn(II) complexes contain extraneous UV absorptions attributable to Cu(II) (and possibly other) impurities. Cu(ImH)<sub>4</sub>SO<sub>4</sub>,<sup>16</sup> bis[cyclo-(L-histidyl-L-histidyl)]copper(II) diperchlorate tetrahydrate (C<sub>12</sub>H<sub>14</sub>N<sub>6</sub>O<sub>2</sub>Cu·2ClO<sub>4</sub>·4H<sub>2</sub>O),<sup>17</sup> aquo- $\mu$ -bis[cyclo-(L-histidyl-L-histidyl)]dicopper(II)

diperchloratemonohydrate (H<sub>2</sub>O(C<sub>12</sub>H<sub>13</sub>N<sub>6</sub>O<sub>2</sub>)<sub>2</sub>Cu<sub>2</sub>·2ClO<sub>4</sub>),<sup>18</sup> [Cu( $\beta$ -ala-L-his)H<sub>2</sub>O]<sub>2</sub>,<sup>19</sup> Cu<sub>3</sub>(ImH)<sub>8</sub>(Im)<sub>2</sub>·4ClO<sub>4</sub>,<sup>20</sup> and Zn(L-His)<sub>2</sub>·2H<sub>2</sub>O<sup>21</sup> were prepared according to published procedures. The densities of these complexes were measured in CCl<sub>4</sub>-BrCH<sub>2</sub>CH<sub>2</sub>Br gradients and compared with the values calculated from the published unit cell parameters. Agreement of the observed and calculated densities within 0.02 g/cm<sup>3</sup> indicated that the synthetic procedures yielded the above complexes. Zn(L-His)<sub>2</sub>·2H<sub>2</sub>O was recrystallized five times from water. Even though the ligands already were in pure form, additional purification of the complex was required to attenuate the extraneous UV absorptions resulting from Cu(II) present in ZnSO<sub>4</sub>·7H<sub>2</sub>O.

The imidazolate-bridged species Im(CuR<sub>2</sub>NCH<sub>2</sub>CH<sub>2</sub>NH-CH<sub>2</sub>CH<sub>2</sub>NR<sub>2</sub>)<sub>2</sub>·3ClO<sub>4</sub> (R = H) was prepared by a published procedure.<sup>22</sup> The Cu-Im<sup>-</sup>-Cu unit recently has been verified by a crystallographic study of a complex where R = CH<sub>3</sub>.<sup>23</sup> The corresponding complex where R = C<sub>2</sub>H<sub>5</sub> was prepared by adding 1 equiv of NaOH to a methanol solution containing equimolar amounts of Cu(ClO<sub>4</sub>)<sub>2</sub>·6H<sub>2</sub>O, Et<sub>2</sub>N(CH<sub>2</sub>)<sub>2</sub>NH(CH<sub>2</sub>)<sub>2</sub>NEt<sub>2</sub>, and ImH.

Anal. Calcd for Cu<sub>2</sub>C<sub>27</sub>H<sub>61</sub>N<sub>8</sub>Cl<sub>3</sub>O<sub>12</sub>: Cu, 13.76; C, 35.12; H, 6.66; N, 12.14. Found: Cu, 13.79; C, 35.05; H, 6.68; N, 12.12.

**Physical Measurements.** Electronic spectra were recorded on Cary Model 14, 18, and 17 spectrophotometers. The latter instrument has been interfaced with a Tektronix computer. Solid samples were dispersed in mineral oil mulls and KBr pellets for electronic spectral studies. Evaporation of aqueous Cu(ImH)<sub>4</sub>SO<sub>4</sub> on quartz flats yielded blue-violet crystalline films of the complex. The films were composed of elongated rectangular plates which were oriented in approximately the same direction, and exhibited well-resolved electronic spectra. Detailed single-crystal studies were not conducted because their usefulness is limited by the low symmetry of the space group (C<sub>2</sub>/c) in which the complex crystallizes.<sup>16</sup>

### Results and Discussion

**Electronic Structure of Imidazole.** An analysis of Cu(II)-ImH LMCT spectra necessarily must consider the electronic